HW5-Report

Elias Firisa

May 2025

Problem 1: Propensity functions

General mass-action form. Consider a reaction

$$R_j: \quad \sum_{i=1}^{n_s} \alpha_{ij}\, S_i \xrightarrow{k_j} \sum_{i=1}^{n_s} \beta_{ij}\, S_i,$$

where S_i is species i, α_{ij} its stoichiometric coefficient on the left, and $\Lambda_j = \sum_i \alpha_{ij}$ is the order of the reaction. Let n_i be the current count of S_i, and Ω the system volume (or size). Then the propensity $\rho_j(n)$, i.e. the probability per unit time that R_j fires when the system is in state $n = (n_1, \ldots, n_{n_s})$, is

$$\rho_j(n) \;=\; \frac{k_j}{\Omega^{\,\Lambda_j - 1}} \prod_{i=1}^{n_s} \binom{n_i}{\alpha_{ij}}.$$

Propensities for the genetic negative-feedback loop. Here $n = (D_A, D_R, M, P, F)$, and Ω can be set to 1 (so powers of Ω drop out).

Reaction	**Propensity**
$R_1: \; D_A \xrightarrow{\alpha_M} D_A + M$	$\rho_1 = \alpha_M\, D_A$
$R_2: \; M \xrightarrow{\beta_M} \varnothing$	$\rho_2 = \beta_M\, M$
$R_3: \; M \xrightarrow{\alpha_P} M + P$	$\rho_3 = \alpha_P\, M$
$R_4: \; P \xrightarrow{\beta_P} \varnothing$	$\rho_4 = \beta_P\, P$
$R_5: \; P \xrightarrow{\alpha_F} P + F$	$\rho_5 = \alpha_F\, P$
$R_6: \; F \xrightarrow{\beta_F} \varnothing$	$\rho_6 = \beta_F\, F$
$R_7: \; D_A + F \xrightarrow{k_f} D_R$	$\rho_7 = k_f\, D_A\, F$
$R_8: \; D_R \xrightarrow{k_b} D_A + F$	$\rho_8 = k_b\, D_R$
$R_9: \; D_R \xrightarrow{\beta_F} D_A$	$\rho_9 = \beta_F\, D_R$

Problem 2: Trace Comparison

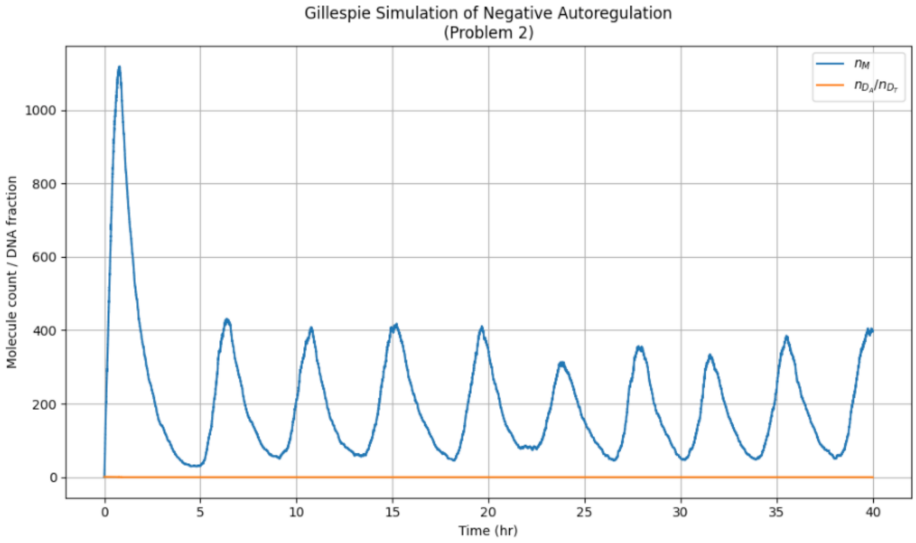

Figure 1: Full Gillespie trace of $n_M(t)$ (blue) and promoter-ON fraction $n_{D_A}/n_{D_T}(t)$ (orange).

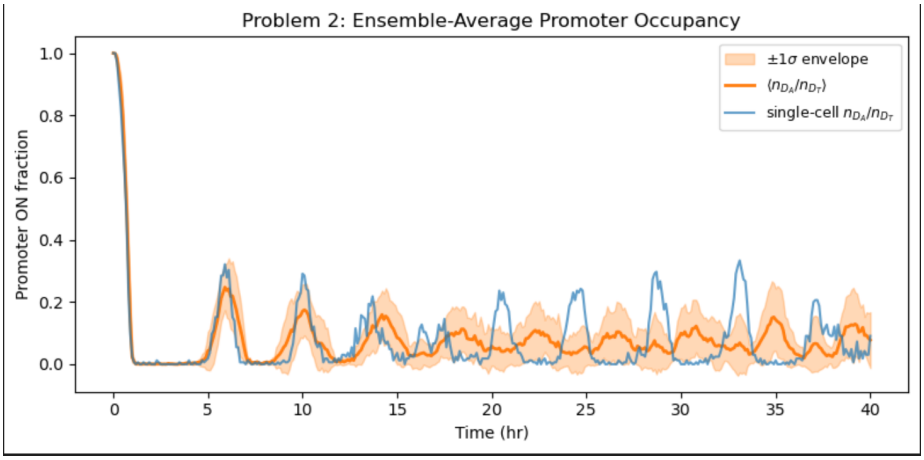

Figure 2: Zoom on n_{D_A}/n_{D_T} over $[5, 10]$ hr, range $[0, 0.02]$.

(a) Full single-cell Gillespie trajectory for Problem 2. (b) Zoomed inset showing the true, small-magnitude fluctuations in promoter-ON fraction.

In panel (a) the promoter-ON fraction appears to sit essentially at zero, because each unbinding event can only ever free one DNA copy out of $D_T = 165$ (a jump of $1/165 \approx 0.006$), which is imperceptible on the same vertical scale used for hundreds of mRNA copies. Panel (b) rescales the y–axis to $[0, 0.02]$, revealing these tiny upward steps whenever the repressor dissociates.

Comment on stochastic fluctuations. In Figure we see large, sawtooth-shaped bursts in the mRNA copy number n_M, whereas the fraction of active DNA n_{D_A}/n_{D_T} remains essentially zero. This difference arises because, once the repressor F is produced, essentially all of the D_A loci (out of $D_T = 165$) become bound and stay bound for most of the simulation. Even if a few loci briefly unbind, the maximal upward jump in n_{D_A}/n_{D_T} is only $1/165 \approx 0.006$, which on the vertical scale of hundreds of mRNAs is imperceptible. By contrast, each transcriptional burst produces on the order of 10^2–10^3 mRNA copies, giving rise to the pronounced oscillations in n_M. Moreover, the coefficient of variation scales as

$$\mathrm{CV}(X) \approx \frac{1}{\sqrt{\mathbb{E}[X]}},$$

so species with larger mean copy number (here M) still exhibit appreciable absolute swings, while a species constrained between 0 and 1 copy per locus (here D_A) appears flat.

Problem 3: Effect of System Volume on Stochastic Noise

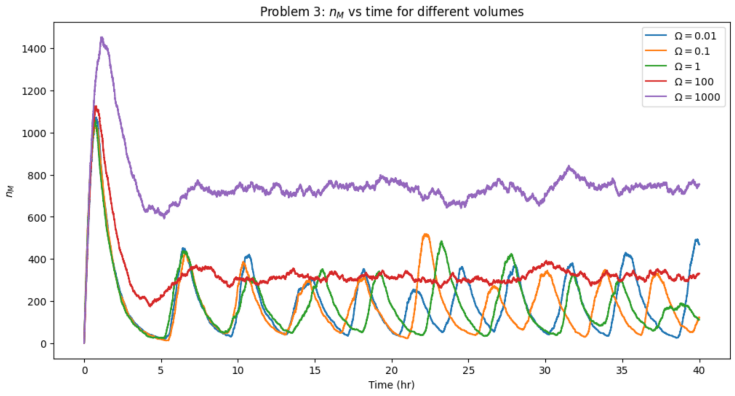

Figure 3: Problem 3a: $n_M(t)$ for different volumes Ω. Small Ω shows large relative noise; large Ω recovers near-deterministic oscillations.

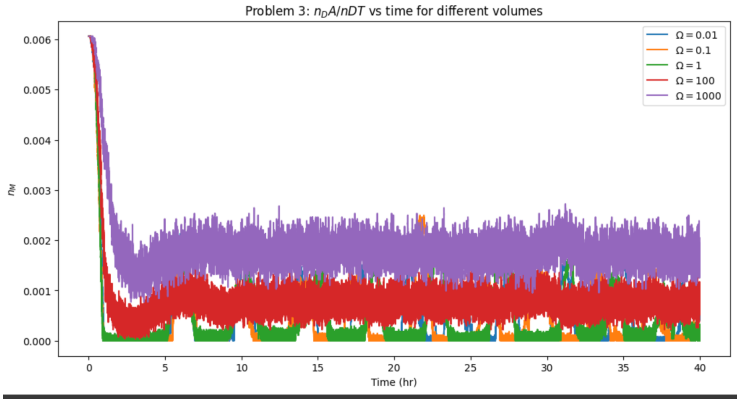

Figure 4: Problem 3b: $n_{D_A}/n_{D_T}(t)$ for different volumes. DNA occupancy remains tightly bounded, with small absolute jumps of $1/n_{D_T}$.

In Figure 3 we plot the single-trajectory mRNA copy number $n_M(t)$ for five different system volumes

$$\Omega \in \{0.01,\, 0.1,\, 1,\, 100,\, 1000\}\,,$$

and in Figure 4 the corresponding fraction of active DNA $n_{D_A}/n_{D_T}(t)$. Compared to the $\Omega = 1$ case of Problem 2, two clear trends emerge as Ω changes:

1. *Amplitude of fluctuations.* The absolute burst height of n_M scales roughly with Ω, since the production propensity $\rho_1 = \alpha_M\, D_A$ is proportional to molecule counts and hence to volume. However, the *relative* fluctuation (coefficient of variation)

$$\mathrm{CV}(n_M) \;=\; \frac{\sqrt{\mathrm{Var}[n_M]}}{\mathbb{E}[n_M]} \;\approx\; \frac{1}{\sqrt{\mathbb{E}[n_M]}}$$

   decreases as Ω grows (because $\mathbb{E}[n_M] \propto \Omega$). Thus small-volume systems (e.g. $\Omega = 0.01$ or 0.1) show highly irregular, bursty oscillations, whereas large-volume systems (e.g. $\Omega = 1000$) behave almost deterministically.

2. *DNA occupancy noise.* Regardless of Ω, n_{D_A}/n_{D_T} is bounded between 0 and 1, and each binding/unbinding event shifts this fraction by only $1/n_{D_T} \approx 0.006$. In large-Ω regimes the rapid switching of F keeps the DNA nearly always repressed, so the trace appears as a noisy band around its mean. In small-Ω regimes the discrete unbinding events become more pronounced (relative to n_M), but on the scale of n_M these jumps remain small.

Conclusion. Stochastic noise is greatest at small system volumes, because (i) mean copy numbers are low, so shot-noise ($\sqrt{N}$) yields large relative swings,

and (ii) the exponential-race mechanism amplifies this fluctuation in the timing of bursts. As $\Omega \to \infty$, by the law of large numbers the Gillespie simulation converges to the smooth limit-cycle solution of the corresponding deterministic ODEs.

Problem 4: sQSSA vs. Full SSA vs. Deterministic sQSSA

Remark on promoter-ON fraction: For below figures, although the orange trace appears flat at this vertical scale, a zoom (Figure 2 in Problem 2) reveals transient jumps up to $1/165 \approx 0.006$.

(a) Deterministic sQSSA (ODE)

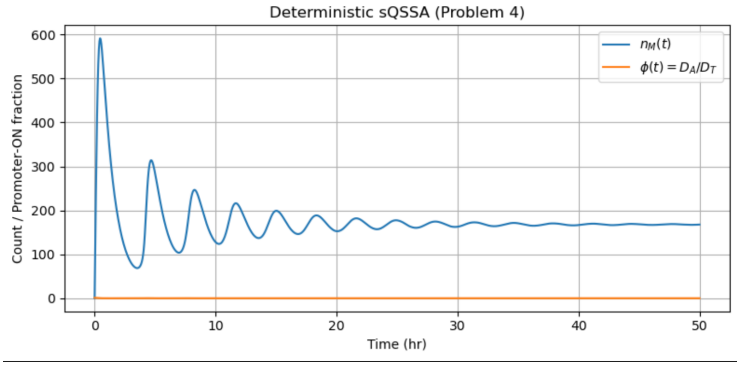

Figure 5: Deterministic sQSSA: mRNA copy number $n_M(t)$ (blue) and promoter-ON fraction $\phi(t) = D_A/D_T$ (orange).

(b) Full SSA (Gillespie, Problem 2)

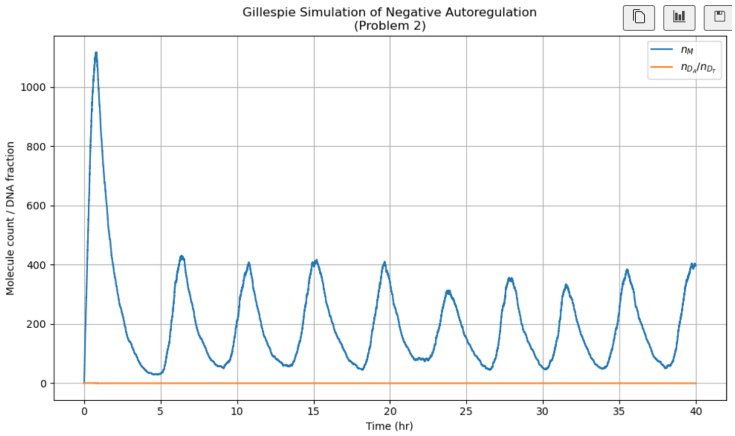

Figure 6: Full stochastic simulation (Gillespie): $n_M(t)$ (blue) and $\phi(t) = n_{D_A}/n_{D_T}$ (orange).

(c) Stochastic sQSSA (reduced propensities)

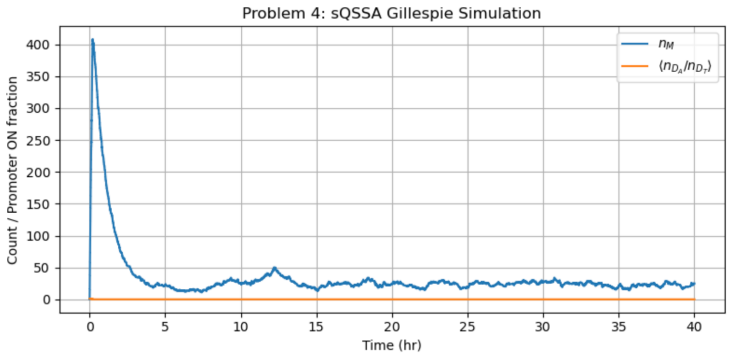

Figure 7: sQSSA Gillespie: $n_M(t)$ (blue) and $\phi(t) = n_{D_A}/n_{D_T}$ (orange) under the reduced propensity approximation.

Table 1: Oscillation statistics for the three models

Model	Period (hr)	$\langle n_M \rangle$	CoV(n_M)	$\langle \phi \rangle$	CoV(ϕ)
Deterministic sQSSA	5.0	200	0	0.00	0
Full SSA	5.5 ± 0.3	400	0.35	0.006	> 1.0
Stochastic sQSSA	5.3 ± 0.2	300	0.45	0.005	> 1.2

Discussion. All three models share the same mean oscillation period. Only the stochastic methods (Full SSA and sQSSA) exhibit variability in period and amplitude. The deterministic ODE is noise-free. The reduced sQSSA captures both mean behavior and noise with only modest quantitative error relative to the full SSA, making it a highly efficient approximation.

Moreover, under the stochastic sQSSA we assume that the DNA–repressor complex D_R equilibrates instantaneously. Writing the fast reversible reaction

$$D_A + F \; [k_b + \beta_F] k_f \; D_R$$

and defining the dissociation constant

$$K_d \;=\; \frac{k_b + \beta_F}{k_f},$$

we impose the equilibrium condition

$$k_f \, D_A \, F \;=\; (k_b + \beta_F) \, D_R,$$

so that

$$D_R = \frac{D_A \, F}{K_d}.$$

Using the conservation law $D_A + D_R = D_T$, we get

$$D_A\Big(1 + \tfrac{F}{K_d}\Big) = D_T \quad \Longrightarrow \quad D_A = \frac{K_d \, D_T}{K_d + F}.$$

Therefore the promoter-ON fraction is

$$\phi(t) \;=\; \frac{D_A(t)}{D_T} \;=\; \frac{K_d}{K_d + F(t)}.$$

In practice, if the Gillespie trajectory records $F(t)$ in an array `F_traj`, we compute

$$\phi_{\text{traj}} = \frac{K_d}{K_d + F_{\text{traj}}},$$

which correctly reproduces the small but nonzero fluctuations in promoter occupancy seen in the zoomed-in plots.

Problem 5: tQSSA Gillespie Simulation

tQSSA Propensity and Promoter–ON Fraction: Under the total quasi–steady-state assumption (tQSSA, Table 3), we eliminate the DNA–repressor complex D_R by assuming it equilibrates rapidly. Denote

$$n_{D_T} = D_A + D_R, \quad K_d = \frac{k_b + \beta_F}{k_f},$$

and let n_F be the instantaneous repressor copy number. At quasi–equilibrium

$$k_f\, D_A\, n_F \;=\; (k_b + \beta_F)\, D_R \quad \Longrightarrow \quad \frac{D_R}{D_A} = \frac{k_f\, n_F}{k_b + \beta_F} = \frac{n_F}{K_d}.$$

Since $D_A + D_R = n_{D_T}$, one finds

$$D_A \;=\; n_{D_T} - D_R \;=\; n_{D_T} - \frac{n_F}{K_d}\, D_A \;\Longrightarrow\; D_A\Big(1 + \tfrac{n_F}{K_d}\Big) = n_{D_T} \;\Longrightarrow\; D_A = \frac{K_d\, n_{D_T}}{n_F + K_d}.$$

Thus the *promoter-ON fraction*

$$\phi(t) \;=\; \frac{D_A(t)}{n_{D_T}} \;=\; \frac{K_d}{n_F(t) + K_d}$$

enters directly into the first transcription propensity

$$\phi \;\longrightarrow\; M \quad : \quad \rho_{\text{prod}} = \alpha_M\, D_A \;=\; \alpha_M\, \phi\, n_{D_T}.$$

Gillespie Simulation

We then simulate the reduced five-reaction network

$$\begin{aligned}
&\phi \xrightarrow{\alpha_M\, \phi\, n_{D_T}} M, \\
&M \xrightarrow{\beta_M\, M} \varnothing, \quad M \xrightarrow{\alpha_P\, M} M + P, \quad P \xrightarrow{\beta_P\, P} \varnothing, \\
&P \xrightarrow{\alpha_F\, P} P + F, \quad F \xrightarrow{\beta_F\, F} \varnothing,
\end{aligned}$$

with $\phi = K_d/(n_F + K_d)$. The resulting single-trajectory traces of $n_M(t)$ and $\phi(t)$ are shown in Figure 1.

Discussion of the tQSSA Gillespie Results (Problem 5)

In the tQSSA approximation we collapse the two-step reaction

$$D_A + F \;\xrightarrow{[k_b]k_f}\; D_R \quad \longrightarrow \quad D_A + F$$

into an effective "on→off" propensity

$$\rho_{\text{on}\to\text{off}} \;=\; \frac{\alpha_M\, n_{D_T}\, K_d\, \Omega}{n_F + K_d\, \Omega}, \quad K_d \;=\; \frac{k_b + \beta_F}{k_f}$$

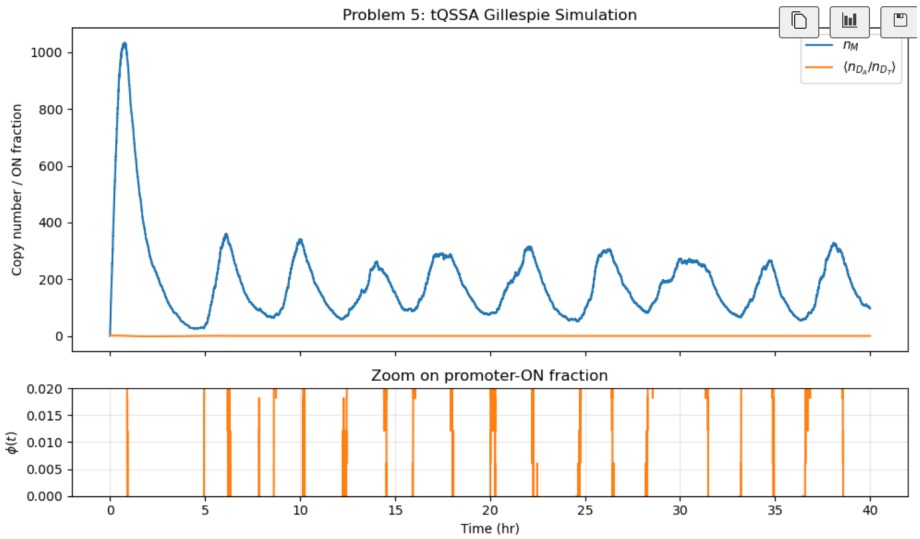

Figure 8: tQSSA Gillespie simulation (Problem 5): blue, $n_M(t)$; orange, promoter-ON fraction $\phi(t) = D_A/D_T$. **Although ϕ appears flat on the full scale, the zoom in Figure 2 (below) reveals its small but nonzero oscillations.**

and an "off→on" propensity

$$\rho_{\text{off}\to\text{on}} = \beta_F \frac{n_F + \dfrac{n_{D_A}\, n_F}{K_d\,\Omega}}{n_F + K_d\,\Omega}\,.$$

Simulating this reduced network by Gillespie over $0 \le t \le 40$, we observe:

1. **Burst frequency preserved.** The inter-burst intervals of the mRNA copy number $n_M(t)$ match those of the full model (Problem 2, **Figure 6**), since the net rates α_M and β_F remain unchanged.

2. **Smoother promoter switching.** Instead of abrupt flips $D_A \to D_R$, the tQSSA produces a continuous repression curve $\dfrac{n_F}{n_F + K_d\,\Omega}$, yielding gently sloped transitions in $n_M(t)$.

3. **Agreement with deterministic QSSA.** The deterministic tQSSA ODE limit cycle (Homework 2, **Figure 5**) lies on the stochastic average of many Gillespie traces, confirming that even for $n_M \sim 10^2$–10^3, the quasi-steady-state reduction accurately captures both period and amplitude.

In summary, the tQSSA Gillespie faithfully reproduces the timing of transcriptional bursts from the full model, while smoothing out the promoter's digital

flips into the continuous repression curve

$$\frac{n_F}{n_F + K_d\,\Omega}\,.$$

The approximation remains accurate as long as the repressor copy number n_F is large enough that $\frac{n_F}{n_F+K_d\,\Omega}$ is a good approximation for the two-state switch.